

# Concerted Asynchronous Hula-Twist Photoisomerization in the S65T/H148D Mutant of Green Fluorescent Protein\*\*

Qiangqiang Zhang, Xuebo Chen,\* Ganglong Cui, Wei-Hai Fang, and Walter Thiel\*

Dedicated to the MPI für Kohlenforschung on the occasion of its centenary

**Abstract:** Fluorescence emission of wild-type green fluorescent protein (GFP) is lost in the S65T mutant, but partly recovered in the S65T/H148D double mutant. These experimental findings are rationalized by a combined quantum mechanics/molecular mechanics (QM/MM) study at the QM(CASPT2//CASSCF)/AMBER level. A barrierless excited-state proton transfer, which is exclusively driven by the Asp148 residue introduced in the double mutant, is responsible for the ultrafast formation of the anionic fluorescent state, which can be deactivated through a concerted asynchronous hula-twist photoisomerization. This causes the lower fluorescence quantum yield in S65T/H148D compared to wild-type GFP. Hydrogen out-of-plane motion plays an important role in the deactivation of the S65T/H148D fluorescent state.

Green fluorescent proteins (GFPs) have become a powerful live-cell imaging tool as biomarkers that monitor cellular processes of living systems in molecular and cellular biology.<sup>[1]</sup> In the past decades, a broad range of GFP variants have been developed, but their brightness and stability are still not optimal. To improve their overall performance, much experimental and theoretical effort is devoted to studying the fundamental working mechanism of GFPs, for instance by varying pH values,<sup>[2]</sup> chemically tailoring chromophores,<sup>[3]</sup> mutating key residues,<sup>[4]</sup> altering hydrogen-bonding networks,<sup>[5]</sup> and locking isomerization channels.<sup>[6]</sup>

Upon photoexcitation of wild-type GFP (wt-GFP), the neutral chromophore *p*-HBDI<sup>[7]</sup> is first deprotonated through a multi-step excited-state proton transfer along the intermolecular hydrogen-bonding network that consists of a water molecule (W22), Ser205, and Glu222.<sup>[8]</sup> This immediately initiates fluorescence emission from the resulting anionic keto intermediate with a fairly high quantum yield (ca. 0.8).<sup>[9]</sup>

Much weaker fluorescence emission in the deuterated GFP protein<sup>[10]</sup> demonstrates that the excited-state proton transfer is a prerequisite to form the fluorescent state.

Tuning excited-state proton transfer processes can significantly change the photophysical and photochemical properties of GFPs. A single S65T mutation leads to the collapse of the original hydrogen-bonding network in wt-GFP; accordingly, the fluorescence quantum yield decreases to 0.02 because the deprotonated fluorescent state is hardly formed in the absence of an effective proton-transfer wire.<sup>[5,11]</sup> Interestingly, fluorescence emission is recovered in the double S65T/H148D GFP mutant.<sup>[5,11,12]</sup> In this mutant, the original long-range intermolecular hydrogen-bonding network is disrupted due to the S65T mutation; instead, a new and much shorter intermolecular hydrogen bond is generated between the hydroxy group of the *p*-HBDI chromophore and the anionic carboxylate COO<sup>−</sup> group of Asp148 (H148D), which can act as a proton acceptor to deprotonate *p*-HBDI, thus forming the fluorescence-emitting state. An ultrafast single-step excited-state proton transfer has indeed been observed experimentally within 175 fs,<sup>[11,12]</sup> which is faster than that found in wt-GFP (sub-picosecond).<sup>[4,8b]</sup> However, the fluorescence quantum yield significantly decreases from 0.8 in wt-GFP<sup>[9]</sup> to 0.21 in the S65T/H148D mutant.<sup>[11]</sup> The photophysics and photochemistry of this double mutant thus differ considerably from those of wt-GFP and of the single S65T mutant.<sup>[11]</sup>

To enhance our understanding of the GFP fluorescence-emitting state and its deactivation, and thus help design new GFP variants satisfying bioimaging needs, it is desirable to study the intriguing photophysics and photochemistry of the GFP mutant<sup>[5,11,12]</sup> at the atomistic level. For this purpose, we use state-of-the-art electronic structure calculations. There have been several quantum-chemical studies focusing on GFP photophysics and photochemistry;<sup>[13]</sup> however, none of them addressed the S65T/H148D double mutant.

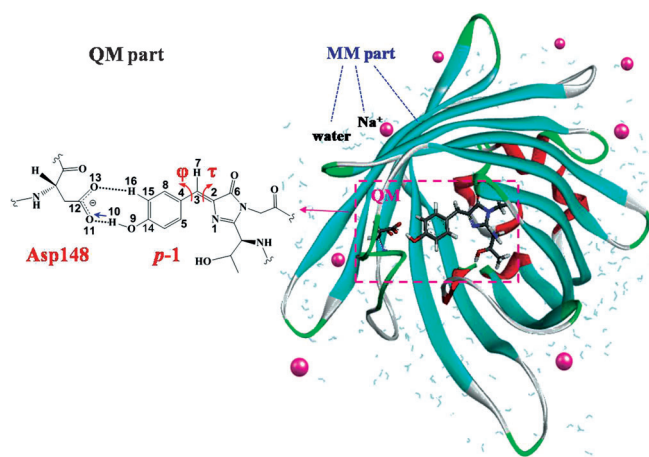
Here, we report QM/MM calculations at the QM(CASPT2//CASSCF)/AMBER level to explore the minimum-energy paths of the S65T/H148D double mutant that are relevant to the ultrafast formation of the anionic fluorescent state and to its deactivation by photoisomerization (Scheme 1) using predefined reaction coordinates (see Supporting Information). For comparison, we also report QM-only calculations on the chosen QM subsystem denoted as “in vacuo” (see Supporting Information for computational details). Both at the QM/MM and QM-only levels, the Asp148 residue in the double mutant is solely responsible for the ultrafast formation of the fluorescent state through

[\*] Dr. Q. Zhang, Prof. X. Chen, Prof. W. Fang  
Key Laboratory of Theoretical and Computational Photochemistry of  
the Chinese Ministry of Education  
Chemistry College, Beijing Normal University  
Beijing 100875 (China)  
E-mail: xuebochen@bnu.edu.cn

Dr. G. Cui, Prof. Dr. W. Thiel  
Max-Planck-Institut für Kohlenforschung  
Kaiser-Wilhelm-Platz 1, 45470 Mülheim an der Ruhr (Germany)  
E-mail: thiel@kofo.mpg.de

[\*\*] This work has been supported by the grants NCET-11-0030 and NSFC21373029 (X.C.), NSFC20720102038 and 2004CB719903 (W.F.).

Supporting information for this article is available on the WWW under <http://dx.doi.org/10.1002/anie.201405303>.



**Scheme 1.** QM/MM computational protocol: The QM subsystem (left) includes the *para*-chromophore (*p*-1) and Asp148. The MM subsystem comprises the remaining amino acid residues, counterions, and water molecules. The key rotations around the P-bond ( $\phi$ ) and the I-bond ( $\tau$ ) are indicated in red. Broken covalent bonds separating the QM and MM regions are saturated using hydrogen link atoms (wavy lines). See Supporting Information for further details.

a barrierless excited-state proton transfer. However, the subsequent deactivation of the *p*-HBDI chromophore changes from a one-bond-flip to a concerted asynchronous hula-twist mechanism when including the MM protein environment (i.e., going from QM-only to QM/MM). This exemplifies the importance of properly accounting for environmental effects in such mechanistic studies.

The electronic transition to the bright  $S_1$  state is of  $\pi\pi^*$  character. The vertical excitation energy is computed to be  $71.1 \text{ kcal mol}^{-1}$  (402 nm) in the double mutant, which is close to the experimentally measured maximum of the absorption band at 411–415 nm.<sup>[2,5,12]</sup> The  $S_0 \rightarrow S_1$  transition leads to a decrease of the state dipole moment from 40.5 D in  $S_0$  to 35.0 D in  $S_1$ . The photoinduced charge relocation slightly

diminishes the negative charge at the O9 atom, from  $-0.76$  in  $S_0$  to  $-0.72$  in  $S_1$ , and reinforces the intermolecular H10...O11 hydrogen bond ( $1.77 \text{ \AA}$  at the  $S_0$  enol minimum vs.  $1.72 \text{ \AA}$  at the  $S_1$  enol minimum). These electronic changes facilitate the subsequent excited-state proton transfer process.

The deprotonation of the *p*-HBDI chromophore by the  $\text{COO}^-$  group of Asp148 (i.e., the excited-state proton transfer) is computed to be barrierless in the  $S_1$  state. Upon irradiation, the H10 proton rapidly migrates along a downhill relaxation pathway to form a chemical bond with the carboxylate O11 atom of Asp148, thus generating the fluorescent state (see the left panel of Figure 1a). In this process, some negative charge is transferred from the O9 atom to the phenyl moiety, and the C14–O9 bond is shortened from  $1.32$  to  $1.27 \text{ \AA}$ , resulting in an  $S_1$  keto tautomer of benzoquinone character. Additionally, this excited-state proton transfer process is predicted to be highly exothermic, with the relative energy decreasing from  $71.1 \text{ kcal mol}^{-1}$  at the Franck–Condon point to  $48.3 \text{ kcal mol}^{-1}$  at the  $S_1$  keto tautomer. This suggests that the excited-state proton transfer will be ultrafast in the S65T/H148D GFP mutant, which is fully consistent with the sub-175 femtosecond timescale

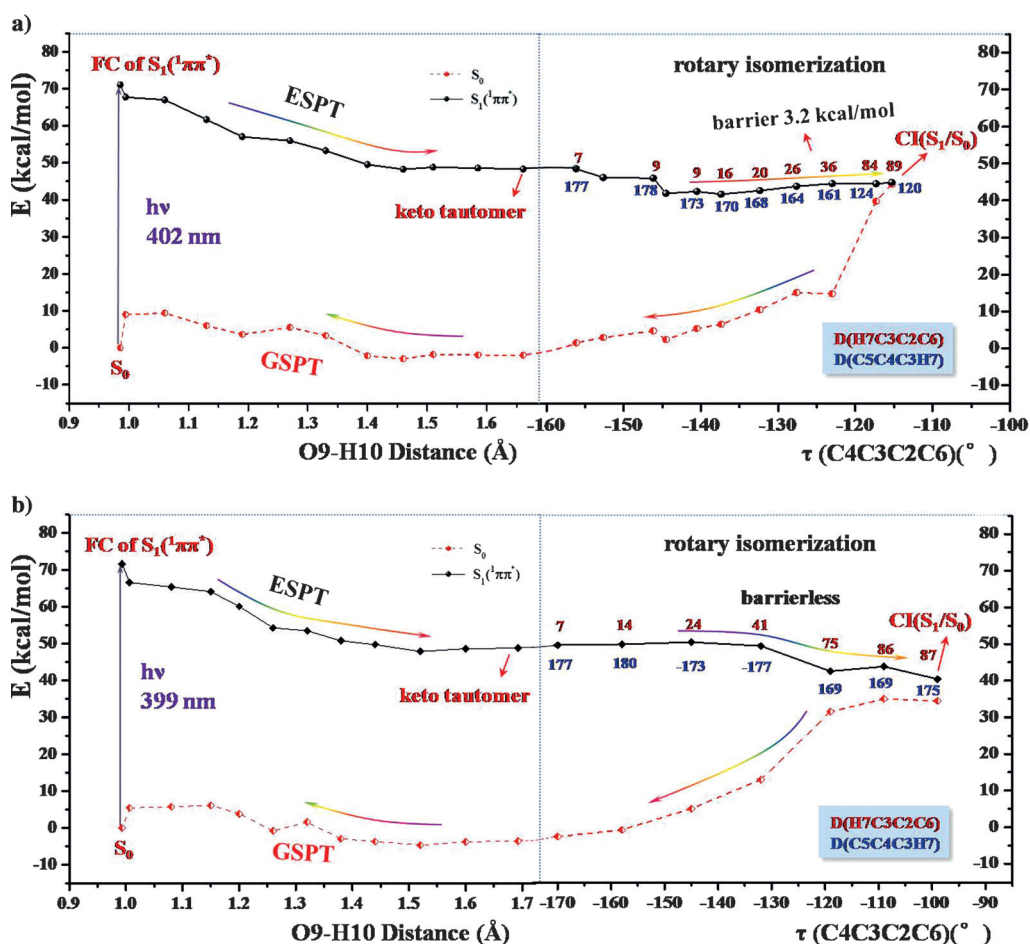


**Figure 1.** Minimum-energy profiles (relaxed  $S_1$  state and unrelaxed  $S_0$  state) along the O9-H10 proton transfer and C4-C3-C2-C6 ( $\tau$ ) isomerization reaction coordinates in the S65T/H148D mutant (a) and in vacuo (b). Also shown are the C5-C4-C3-H7 and H7-C3-C2-C6 dihedral angles. CI, conical intersection; FC, Franck–Condon point; ESPT, excited-state proton transfer; GSPT, ground-state proton transfer.

observed experimentally,<sup>[11,12]</sup> and qualitatively different from the situation in wt-GFP where a small barrier has to be overcome so that the corresponding proton transfer time is delayed into a picosecond time window.<sup>[4,8b]</sup> There are two reasons for this difference. First, the deprotonation of the *p*-HBDI chromophore (acting as a photoacid) in the double mutant is barrierless, and the proton transfer to the Asp148 carboxylate is very exoergic. Second, kinetically, excited-state proton transfer is a single-step, two-body (Asp148 and *p*-HBDI), barrierless process in the S65T/H148D mutant, whereas in wt-GFP it is a multi-step, four-body process (W22, Ser205, Glu222, and *p*-HBDI) that has to surmount a non-negligible barrier.<sup>[5,12]</sup>

Another finding is that the excited-state proton transfer path in the protein is virtually the same as that in vacuo (Figure 1), thereby further confirming that the deprotonated Asp148 provides the only driving force for the ultrafast proton transfer observed in the S65T/H148D mutant. By contrast, as discussed in the following, the protein surrounding completely alters the path for the subsequent deactivation.

In vacuo, the  $S_1$  deactivation occurs by isomerization through the classical one-bond flip (OBF) mechanism. This isomerization proceeds mainly through rotation around the C4-C3-C2-C6 ( $\tau$ ) dihedral angle (from  $-175^\circ$  to  $-99^\circ$ ), which is nearly synchronous with the H7-C3-C2-C6 rotation (see the right panel of Figure 1b). As expected, the C5-C4-C3-H7 dihedral angle remains close to  $\pm 180^\circ$  during the whole excited-state relaxation process. The geometric structure of the approximate  $S_1/S_0$  conical intersection further supports the OBF mechanism (Figure 2b), with nearly perpendicular

C4-C3-C2-C6 and H7-C3-C2-C6 dihedral angles (i.e.  $-99^\circ$  and  $87^\circ$ ) and almost planar C5-C4-C3-C2 and C5-C4-C3-H7 arrangements. Energetically, this excited-state isomerization is barrierless and eventually leads to an  $S_1/S_0$  conical intersection region; the minimum  $S_1-S_0$  energy gap on this pathway was found to be  $6.0 \text{ kcal mol}^{-1}$  at the CASPT2//CASSCF level. Thus, this deactivation channel can be easily accessed, which is consistent with the ultralow fluorescence quantum yield that is observed in vacuo and in dilute solution.<sup>[13]</sup>

In the S65T/H148D mutant, the deactivation of the  $S_1$  state becomes more complicated because of the complex protein surrounding. A one-bond flip mechanism with rotation around the P-bond (C5-C4-C3-C2,  $\phi$ ) is not allowed energetically. The calculated minimum-energy reaction path for the *p*-HBDI chromophore along this reaction coordinate is shown in Figure S1 in the Supporting Information. When the dihedral angle gradually increases from  $-11^\circ$  to  $105^\circ$ , the intermolecular O9...H10 hydrogen bond is slightly elongated from 1.66 to 1.70 Å, while the O13...H16 distance drastically increases from 2.92 to 3.89 Å. To achieve such a pronounced conformational change from the stable  $S_1$  keto tautomer, a large barrier ( $> 40 \text{ kcal mol}^{-1}$ ) needs to be overcome. This differs from the situation in vacuo.<sup>[13]</sup> Furthermore, along this C5-C4-C3-C2 ( $\phi$ ) torsion, we do not find an energetically degenerate  $S_1/S_0$  conical intersection region, with the smallest computed  $S_1-S_0$  energy gap being  $23.5 \text{ kcal mol}^{-1}$ . Thus, an isomerization only involving the C5-C4-C3-C2 ( $\phi$ ) torsional reaction coordinate, that is, the one-bond flip mechanism, appears to be prohibited in the S65T/H148D GFP mutant.

An alternative mechanism for the photoisomerization involves the volume-conserving hula-twist motion.<sup>[14]</sup> It requires correlated rotations around the P-bond and the I-bond, otherwise it degrades to a simple one-bond flip motion as the case just discussed, where the C4-C3-C2-C6 ( $\tau$ ) dihedral angle related to I-bond rotation merely varies by several degrees. However, in terms of the temporal sequence, the hula-twist motion around the P- and I-bonds may happen synchronously or asynchronously.

We first optimized the minimum-energy profile for synchronous hula-twist motion, with simultaneous rotation around the C5-C4-C3-C2 ( $\phi$ ) and C4-C3-C2-C6 ( $\tau$ ) dihedral angles, that is, P- and I-bond rotation. In these constrained optimizations, the two dihedral angles were gradually twisted to ca.  $80^\circ$  (see Figure S2). Along this minimum-energy path, the dihedral angle (C5-C4-C3-H7) associated with the central C-H moiety is twisted out of the plane of the two rings by more than  $45^\circ$ . Similar to the OBF case (see above), the O13...H16 distance is remarkably elongated to 3.72 Å (from 2.92 Å in the  $S_1$  keto tautomer), and there is a significant barrier ( $> 36 \text{ kcal mol}^{-1}$ ). Hence, the synchronous hula-twist mechanism with simultaneous rotation around the P- and I-bonds can also not be responsible for the low fluorescence quantum yield (0.2) observed in the S65T/H148D GFP mutant.<sup>[11]</sup> At the end point of this path (i.e., at  $\phi = 77^\circ$ ), there is still an  $S_1-S_0$  energy gap of  $10.8 \text{ kcal mol}^{-1}$ , which is however much smaller than the gap of  $23.5 \text{ kcal mol}^{-1}$  found for the one-bond ( $\phi$ ) flip mechanism.

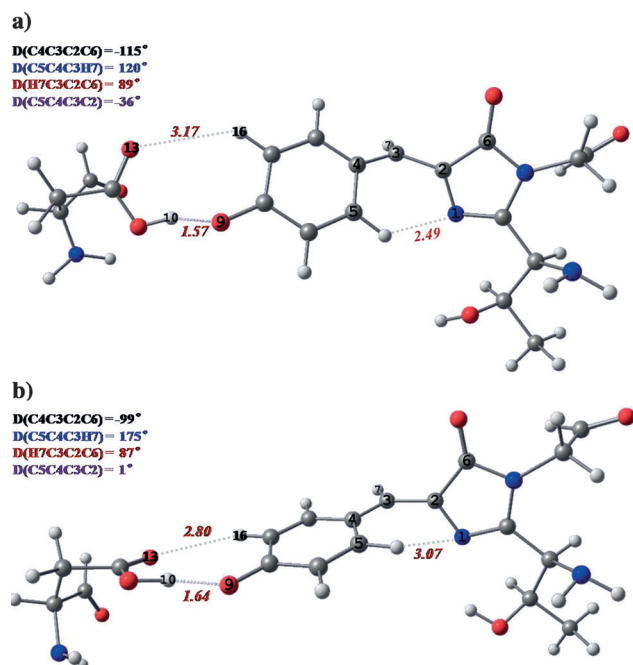


**Figure 2.** Schematic structures of the  $S_1/S_0$  conical intersections related to photoisomerization (a) in the S65T/H148D GFP mutant and (b) in vacuo (dihedral angles  $D$  in degree and distances in Ångström).



Motivated by the small gap on the synchronous hula-twist path, we further explored the possibility of an asynchronous hula-twist motion. In the optimizations along this asynchronous path, only the C4-C3-C2-C6 ( $\tau$ ) dihedral angle was fixed at each point. As shown in Figure 1 a, when the C4-C3-C2-C6 ( $\tau$ ) dihedral angle in the double mutant changes from  $-164^\circ$  in the  $S_1$  keto tautomer to  $-115^\circ$  at the  $S_1/S_0$  conical intersection, the corresponding H7-C3-C2-C6 dihedral angle affiliated with the central CH moiety increases as well from  $7^\circ$  to  $89^\circ$ . These changes are quite similar to those in vacuo (OBF, Figure 1 b), except for the qualitatively different behavior of the C5-C4-C3-H7 dihedral angle: in the S65T/H148D GFP mutant, this dihedral angle decreases to  $120^\circ$  (from  $178^\circ$  in the  $S_1$  keto tautomer), whereas it always remains close to  $\pm 180^\circ$  in vacuo. Similar structural features are found at the  $S_1/S_0$  conical intersection in the double mutant (see Figure 2 a), in which the two rings are nearly coplanar but the central CH unit is strongly twisted out of this plane (see Table S4).

Contrary to the synchronous hula-twist isomerization, the concerted asynchronous hula-twist pathway is energetically allowed in the S65T/H148D GFP mutant. When going from the  $S_1$  enol minimum to the  $S_1$  keto tautomer, the C3-C4/C2-C3 bond length increases/decreases from 1.40/1.49 to 1.45/1.46 Å (see Table S4). The computed barrier of  $3.2 \text{ kcal mol}^{-1}$  on the minimum-energy path is quite small (Figure 1 a), and there is an  $S_1/S_0$  conical intersection, which is  $26.2 \text{ kcal mol}^{-1}$  lower in energy than the  $S_1(^1\pi\pi^*)$  state at the Franck–Condon point. The system will thus be able to decay to the  $S_0$  state via this funnel. Therefore, the S65T/H148D GFP mutant will follow the concerted asynchronous hula-twist isomerization path to de-excite the  $S_1$  keto tautomer.

On this pathway, the hydrogen-out-of-plane motion (HOOP, H7 atom) plays an important role in lowering the isomerization barrier in the rigid protein surrounding. This is reflected in the HOOP dihedral angle of  $120^\circ$  at the  $S_1/S_0$  conical intersection of the double mutant (see Figure 2 a). Such HOOP motion has previously been reported in the photoisomerization of the chromophores of rhodopsin<sup>[15]</sup> and photoactive yellow proteins<sup>[16]</sup> as well as in photochromic spiropyran<sup>[17]</sup> (but, to our knowledge, not yet in GFPs). We emphasize that the HOOP motion in the central CH unit does not occur in vacuo, but only in the S65T/H148D double mutant during the late stages of the photoisomerization (see Section 2.3 in the Supporting Information). The strong HOOP distortion (twist  $> 60^\circ$ , see Figure 2 a) raises the  $S_0$  energy and gives rise to the  $S_1/S_0$  conical intersection. It is necessitated by the rigid cavity near the GFP chromophore: there are strong steric interactions with adjacent residues in the double mutant, which prohibit the one-bond flip photoisomerization (preferred in vacuo) and instead favor a volume-conserving hula-twist mechanism combined with HOOP motion in the central CH moiety.

Despite the ultrafast formation of the fluorescent state and the energetically accessible conical intersection, the  $S_1$  deactivation should be less efficient in the double mutant than in vacuo, since there is a small isomerization barrier of ca.  $3 \text{ kcal mol}^{-1}$  in the protein environment. The S65T/H148D double mutant fluoresces brightly because the chromophore-

Asp148 hydrogen bond enables an ultrafast sub-175 fs excited-state proton transfer forming the fluorescence-emitting  $S_1$  keto state, which is long-lived enough to give a fluorescence quantum yield of 0.21,<sup>[11]</sup> less than in wt-GFP (0.8)<sup>[9]</sup> but much higher than in the S65T mutant (0.02).<sup>[11]</sup> As explained above, these differences can be attributed to different topologies of the  $S_1$  potential energy surfaces.

We emphasize that the value of ca.  $3 \text{ kcal mol}^{-1}$  for the barrier is only a rough estimate from a reaction path calculation for one particular protein conformation. Without claiming any quantitative accuracy, we focus on the qualitative feature of having a small barrier for isomerization. Without such a barrier, one would expect an ultrafast deactivation of the fluorescent  $S_1$  keto state (no fluorescence), while a high barrier would trap this state and lead to high fluorescence. Qualitatively, the existence of a small barrier is compatible with the observed fluorescence quantum yield of 0.21.<sup>[11]</sup>

To summarize, we have employed ab initio QM-only and QM/MM methods to explore the ultrafast formation of the fluorescent state and its deactivation in the S65T/H148D GFP mutant. We found that Asp148 provides the exclusive driving force for the ultrafast sub-175 fs formation of the fluorescent state, which is little affected by the protein surrounding. By contrast, the environment completely changes the deactivation path of the fluorescent state ( $S_1$  keto tautomer), from a one-bond-flip mechanism in vacuo to a hula-twist mechanism in the double mutant. Closer analysis of minimum-energy profiles shows that the favored hula-twist pathway involves concerted asynchronous motion and strongly benefits from simultaneous HOOP motion in the final stage of the photoisomerization. These insights provide a detailed understanding of the hula-twist photoisomerization mechanism and its specific features in GFP. On the methodological side, the present work confirms that the QM/MM method<sup>[18]</sup> is suitable for studying the photophysics and photochemistry of biological systems<sup>[19]</sup> as complex as the S65T/H148D GFP mutant where the protein environment plays a decisive role in tuning and choreographing excited-state proton transfer and isomerization processes.

Received: May 15, 2014

Published online: July 14, 2014

**Keywords:** green fluorescent protein · hula-twist · photoisomerization · proton transfer · QM/MM

- [1] a) M. Chalfie, Y. Tu, G. Euskirchen, W. W. Ward, D. C. Prasher, *Science* **1994**, 263, 802–805; b) G. U. Nienhaus, *Angew. Chem.* **2008**, 120, 9130–9132; *Angew. Chem. Int. Ed.* **2008**, 47, 8992–8994; c) O. Shimomura, *Angew. Chem.* **2009**, 121, 5698–5710; *Angew. Chem. Int. Ed.* **2009**, 48, 5590–5602; d) M. Chalfie, *Angew. Chem.* **2009**, 121, 5711–5720; *Angew. Chem. Int. Ed.* **2009**, 48, 5603–5611; e) R. Y. Tsien, *Angew. Chem.* **2009**, 121, 5721–5736; *Angew. Chem. Int. Ed.* **2009**, 48, 5612–5626; f) A. B. Cubitt, R. Heim, S. R. Adams, A. E. Boyd, L. A. Gross, R. Y. Tsien, *Trends Biochem. Sci.* **1995**, 20, 448–455; g) R. Y. Tsien, *Annu. Rev. Biochem.* **1998**, 67, 509–544; h) M. Zimmer, *Chem. Rev.* **2002**, 102, 759–781.

- [2] M. A. Elsliger, R. M. Wachter, G. T. Hanson, K. Kallio, S. J. Remington, *Biochemistry* **1999**, *38*, 5296–5301.
- [3] K. Y. Chen, Y. M. Cheng, C. H. Lai, C. C. Hsu, M. L. Ho, G. H. Lee, P. T. Chou, *J. Am. Chem. Soc.* **2007**, *129*, 4534–4535.
- [4] D. Stoner-Ma, A. A. Jaye, P. Matousek, M. Towrie, S. R. Meech, P. J. Tonge, *J. Am. Chem. Soc.* **2005**, *127*, 2864–2865.
- [5] D. Stoner-Ma, A. A. Jaye, K. L. Ronayne, J. Nappa, S. R. Meech, P. J. Tonge, *J. Am. Chem. Soc.* **2008**, *130*, 1227–1235.
- [6] M. S. Baranov, K. A. Lukyanov, A. O. Borissova, J. Shamir, D. Kosenkov, L. V. Slipchenko, L. M. Tolbert, I. V. Yampolsky, K. M. Solntsev, *J. Am. Chem. Soc.* **2012**, *134*, 6025–6032.
- [7] Full chemical name: 4-(4-hydroxybenzylidene)-1,2-dimethyl-1*H*-imidazol-5(4*H*)-one.
- [8] a) K. Brejc, T. K. Sixma, P. A. Kitts, S. R. Kain, R. Y. Tsien, M. Ormö, S. J. Remington, *Proc. Natl. Acad. Sci. USA* **1997**, *94*, 2306–2311; b) S. R. Meech, *Chem. Soc. Rev.* **2009**, *38*, 2922–2934; c) C. Fang, R. R. Frontiera, R. Tran, R. A. Mathies, *Nature* **2009**, *462*, 200–204.
- [9] H. Morise, O. Shimomura, F. H. Johnson, J. Winant, *Biochemistry* **1974**, *13*, 2656–2662.
- [10] P. Leiderman, L. Genosar, D. Huppert, X. Shu, S. J. Remington, K. M. Solntsev, L. M. Tolbert, *Biochemistry* **2007**, *46*, 12026–12036.
- [11] X. Shu, K. Kallio, X. Shi, P. Abbyad, P. Kanchanawong, W. Childs, S. G. Boxer, S. J. Remington, *Biochemistry* **2007**, *46*, 12005–12013.
- [12] a) X. Shi, P. Abbyad, X. Shu, K. Kallio, P. Kanchanawong, W. Childs, S. J. Remington, S. G. Boxer, *Biochemistry* **2007**, *46*, 12014–12025; b) M. Kondo, I. A. Heisler, D. Stoner-Ma, P. J. Tonge, S. R. Meech, *J. Am. Chem. Soc.* **2010**, *132*, 1452–1453.
- [13] a) W. Weber, V. Helms, J. A. McCammon, P. W. Langhoff, *Proc. Natl. Acad. Sci. USA* **1999**, *96*, 6177–6182; b) M. E. Martin, F. Negri, M. Olivucci, *J. Am. Chem. Soc.* **2004**, *126*, 5452–5464; c) A. Sinicropi, T. Andruniow, N. Ferré, R. Basosi, M. Olivucci, *J. Am. Chem. Soc.* **2005**, *127*, 11534–11535; d) P. Altoe, F. Bernardi, M. Garavelli, G. Orlandi, F. Negri, *J. Am. Chem. Soc.* **2005**, *127*, 3952–3963; e) S. Olsen, S. C. Smith, *J. Am. Chem. Soc.* **2007**, *129*, 2054–2065; f) A. M. Virshup, C. Punwong, T. V. Pogorelov, B. A. Lindquist, C. Ko, T. J. Martinez, *J. Phys. Chem. B* **2009**, *113*, 3280–3291; g) I. V. Polyakov, B. L. Grigorenko, E. M. Epifanovsky, A. I. Krylov, A. V. Nemukhin, *J. Chem. Theory Comput.* **2010**, *6*, 2377–2387; h) G. L. Cui, Z. G. Lan, W. Thiel, *J. Am. Chem. Soc.* **2012**, *134*, 1662–1672.
- [14] a) R. S. H. Liu, D. T. Browne, *Acc. Chem. Res.* **1986**, *19*, 42–48; b) A. M. Müller, S. Lochbrunner, W. E. Schmid, W. Fuß, *Angew. Chem.* **1998**, *110*, 520–522; *Angew. Chem. Int. Ed.* **1998**, *37*, 505–507; c) R. S. H. Liu, G. S. Hammond, *Chem. Eur. J.* **2001**, *7*, 4536–4544; d) R. S. H. Liu, *Acc. Chem. Res.* **2001**, *34*, 555–562; e) Y. Imamoto, T. Kuroda, M. Kataoka, S. Shevyakov, G. Krishnamoorthy, R. S. H. Liu, *Angew. Chem.* **2003**, *115*, 3758–3761; *Angew. Chem. Int. Ed.* **2003**, *42*, 3630–3633; f) S. Schieffer, J. Pescatore, R. Ulsh, R. S. H. Liu, *Chem. Commun.* **2004**, 2680–2681; g) R. S. H. Liu, G. S. Hammond, *Acc. Chem. Res.* **2005**, *38*, 396–403.
- [15] a) P. Kukura, D. W. McCamant, S. Yoon, D. B. Wandschneider, R. A. Mathies, *Science* **2005**, *310*, 1006–1009; b) I. Schapiro, M. N. Ryazantsev, L. M. Frutos, N. Ferré, R. Lindh, M. Olivucci, *J. Am. Chem. Soc.* **2011**, *133*, 3354–3364; c) L. M. Frutos, T. Andruniow, F. Santoro, N. Ferré, M. Olivucci, *Proc. Natl. Acad. Sci. USA* **2007**, *104*, 7764–7769; d) N. Klaffki, O. Weingart, M. Garavelli, E. Spohr, *Phys. Chem. Chem. Phys.* **2012**, *14*, 14299–14305.
- [16] E. V. Gromov, I. Burghardt, H. Köppel, L. S. Cederbaum, *J. Phys. Chem. A* **2011**, *115*, 9237–9248.
- [17] F. Y. Liu, K. Morokuma, *J. Am. Chem. Soc.* **2013**, *135*, 10693–10702.
- [18] a) A. Warshel, M. Levitt, *J. Mol. Biol.* **1976**, *103*, 227–249; b) M. J. Field, P. A. Bash, M. Karplus, *J. Comput. Chem.* **1990**, *11*, 700–733; c) H. M. Senn, W. Thiel, *Angew. Chem.* **2009**, *121*, 1220–1254; *Angew. Chem. Int. Ed.* **2009**, *48*, 1198–1229.
- [19] a) A. Toniolo, G. Granucci, T. J. Martinez, *J. Phys. Chem. A* **2003**, *107*, 3822–3830; b) M. Ruckebauer, M. Barbatti, B. Sellner, T. Müller, H. Lischka, *J. Phys. Chem. A* **2010**, *114*, 12585–12590; c) M. Böckmann, N. L. Doltsinis, D. Marx, *J. Phys. Chem. A* **2010**, *114*, 745–754; d) M. E. Moret, I. Tavernelli, U. Rothlisberger, *J. Phys. Chem. B* **2009**, *113*, 7737–7744; e) Y. Lu, Z. G. Lan, W. Thiel, *Angew. Chem.* **2011**, *123*, 6996–6999; *Angew. Chem. Int. Ed.* **2011**, *50*, 6864–6867.